Optimization design of the angle detecting system used in the fast steering mirror*

NI Ying-xue (倪迎雪)[1,2]**, **WU Jia-bin** (吴佳彬)[1], **SAN Xiao-gang** (伞晓刚)[1], **GAO Shi-jie** (高世杰)[1], **DING Shao-hang** (丁少行)[1,2], **WANG Jing** (王晶)[1], **WANG Tao** (王涛)[1,2], and **WANG Hui-xian** (王惠先)[3]

1. Changchun Institute of Optics, Fine Mechanics and Physics, Chinese Academy of Sciences, Changchun 130033, China

2. University of Chinese Academy of Sciences, Beijing 100049, China

3. Huaian City Qingjiang Top Bearing Company Limited, Huaian 223300, China

(Received 23 July 2017; Revised 4 September 2017)

In this paper, in order to design a fast steering mirror (FSM) with large deflection angle and high linearity, a deflection angle detecting system (DADS) using quadrant detector (QD) is developed. And the mathematical model describing DADS is established by analyzing the principle of position detecting and error characteristics of QD. Based on this mathematical model, the variation tendencies of deflection angle and linearity of FSM are simulated. Then, by changing the parameters of the DADS, the optimization of deflection angle and linearity of FSM is demonstrated. Finally, a QD-based FSM is designed based on this method, which achieves ±2° deflection angle and 0.72% and 0.68% linearity along *x* and *y* axis, respectively. Moreover, this method will be beneficial to the design of large deflection angle and high linearity FSM.

Document code: A **Article ID:** 1673-1905(2018)01-0048-5

DOI https://doi.org/10.1007/s11801-018-7172-4

On the free-space optical (FSO) communication links, the light beam may deviate from the terminal owing to the external mechanical and atmospheric disturbances, causing communication outage[1]. Thus, it is very necessary to accurately control the transmission direction of light beam. As it is capable of steering light beam fast and precisely, the fast steering mirror (FSM) has been widely applied to the acquisition, pointing and tracking (APT) of FSO system[2]. Besides, it is also applied to some other fields, such as lidar, astronomical telescope and image stabilization[3].

With the tendency of improving acquisition field and tracking precision of APT system, the FSM with large deflection angle and high linearity has recently become a research focus[4]. The deflection angle detecting system (DADS) is used to detect the deflection angle of FSM and provide angle feedback for actuators. Its performance directly affects the deflection angle and linearity of the FSM. Generally, there are a few kinds of deflection angle detecting systems applied to FSM. D. J. Kluk et al[5] designed a high-bandwidth and high-precision FSM using capacitance probe sensor, and HEI Mo et al[6] designed an FSM which used eddy current proximity sensor. However, these two kinds of sensors have relatively small measurement range. In addition, the resistance strain gauge was used to detect deflection angle for FSM, while the serious temperature drift made it difficult to obtain high linearity[7]. Recently, a new FSM has achieved large deflection angle and high linearity simultaneously, which employs the DADS based on lateral effect position sensitive detector (PSD)[3]. However, the performance parameters of PSDs, such as resolution and response, are limited by the fabrication of these devices. Compared with PSD, the QD has the advantages of lower inherent noise and higher resolution, and it has a faster response. Therefore, the QD has been widely applied to the noncontact dimensional measurement at the micrometer scale[8]. Consequently, it is valuable to design the DADS for FSM using relatively simple optical structure based on QD.

In this paper, a QD-based DADS with a simple optical structure is designed for the FSM. We focus on the large deflection angle and high linearity of FSM by optimizing the DADS.

The designed FSM is mainly composed of a major mirror, a flexible hinge support, four voice coil actuators (VCAs), a main casing and the DADS, as shown in Fig.1. The major mirror is stuck to mirror base supported by flexible hinge, which is fixed in the front of the main casing with screws. The magnets of VCAs are mounted on the back of the mirror base and the coils are fixed on the main casing. Two pairs of VCAs mounted perpendicularly drive the FSM to deflect via elastic deformation of the flexible hinge. The deflection angle is detected by DADS, and the angle information of minor mirror is fed back to VCAs simultaneously. Besides, the flexible hinge support

* This work has been supported by the National Natural Science Foundation of China (No.51605465).

** E-mail: ccniyinguxe@163.com

can keep the major mirror in the balanced position, while no voltage is applied to the VCAs.

The DADS is one of the important components of the FSM, which contains a light source (LS), a minor mirror and a QD. As shown in Fig.1, the beam emitted from the light source is reflected by the minor mirror, and then arrives at the QD which is used to detect angle information of minor mirror. LS and QD are mounted symmetrically about the normal of minor mirror. The minor mirror is stuck on the back of the mirror base, and it is in parallel with major mirror so that the deflection angle of the minor mirror is the same as that of the major mirror, so the DADS can be used to detect the deflection angle of the major mirror.

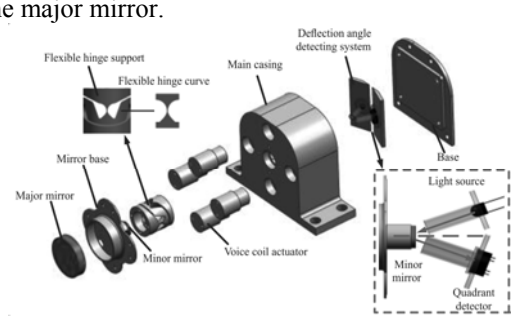

Fig.1 Exploded view of the QD-based FSM

The QD comprises four identical p-n junction photodiodes separated by very small gaps, as shown in Fig.2. With the spot moving on the QD, the position of spot is estimated according to the voltage generated on each photodiode. The spot position estimation is given as

$$\begin{cases} \sigma_x = \psi_{\mathrm{K}} \dfrac{U_{\mathrm{A}} + U_{\mathrm{C}} - U_{\mathrm{B}} - U_{\mathrm{D}}}{U_{\mathrm{A}} + U_{\mathrm{B}} + U_{\mathrm{C}} + U_{\mathrm{D}}}, \\ \sigma_y = \psi_{\mathrm{K}} \dfrac{U_{\mathrm{A}} + U_{\mathrm{B}} - U_{\mathrm{C}} - U_{\mathrm{D}}}{U_{\mathrm{A}} + U_{\mathrm{B}} + U_{\mathrm{C}} + U_{\mathrm{D}}}, \end{cases} \tag{1}$$

where σ_x and σ_y are output signal offsets. ψ_{K} is the proportional coefficient, whose value is related to the spot diameter and energy distribution of the spot[9]. U_{A}, U_{B}, U_{C} and U_{D} are the voltages generated on each photodiode, respectively. Generally, there is high linearity of output position only when the spot is near the QD center, and the linearity increases gradually with the spot being far away from the QD center[10]. The spot position measurement error is defined as $\Delta E_{Lx}=x_0-\sigma_x$, $\Delta E_{Ly}=y_0-\sigma_y$, where (x_0, y_0) is the theoretical position of the spot center and (σ_x, σ_y) is the estimated position. There is a maximal positional error in a certain measurement range. The linearity of detecting the spot position using QD in x-direction is defined as

$$\delta_x = \left|\Delta E_{L\max}\right| \Big/ S, \tag{2}$$

where $|\Delta E_{L\max}|$ denotes the maximum position measurement error, and S is the measurement range.

When the spot is moving on the QD, the spot position can be estimated via Eq.(1). Since the performances of the QD in the two directions are symmetrical, all the following discussions are concentrated on the x-direction for simplification. For the convenience of research, an available 7-mm-diameter QD is used for the analysis and simulation, and the similar conclusion can be also obtained for other sizes of QD.

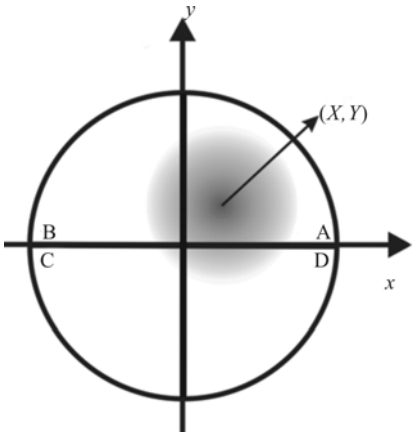

Fig.2 The incident spot on the QD

Assuming that the spot moves on QD from −0.3 mm to +0.3 mm, the spot radii (ω) are supposed to be 3 mm, 4 mm and 5 mm, respectively, and the three curves of position error can be simulated with MATLAB according to Eq.(2), as shown in Fig.3(a). When the spot radii are 3 mm and 5 mm, the corresponding linearities of QD are 0.29% and 0.08% respectively, and the linearity is improved by 72.4%. Therefore, it can be easily seen that the position error decreases gradually with the spot radius increasing at the same position, namely, the linearity will be greatly improved by increasing the spot radius.

Then, supposing that the spot also moves on QD, a series of measurement ranges that satisfy linearity of 1% can be found by constantly changing the size of spot radius. By researching the obtained data, it is discovered that measurement range and spot radii are linearly correlated, and the fitting line is shown in Fig.3(b). The expression of fitting line is given as

$$S_{\mathrm{f}} = a\omega - b, \tag{3}$$

where S_{f} is the fitting measurement range, and a and b are the fitting coefficients. Other fitting lines and corresponding groups of (a, b) also can be obtained in this method when the linearity is changed. We have also acquired a conclusion that the greater the linearity is, the smaller a and b are, and the smaller the measurement range that satisfies the corresponding linearity becomes.

Fig.4 illustrates the working principle of the DADS, and the parameters and symbols are shown in Tab.1. When a Gaussian beam is incident on the QD, with minor mirror deflecting a certain angle (α), we can obtain the deflection angle of the beam ($\beta=2\alpha$) based on the geometrical optics theory. At the same time, the range of spot moving on the QD is given as

$$d_{\mathrm{QD}} = L_{\mathrm{QD}} * \tan 2\alpha. \tag{4}$$

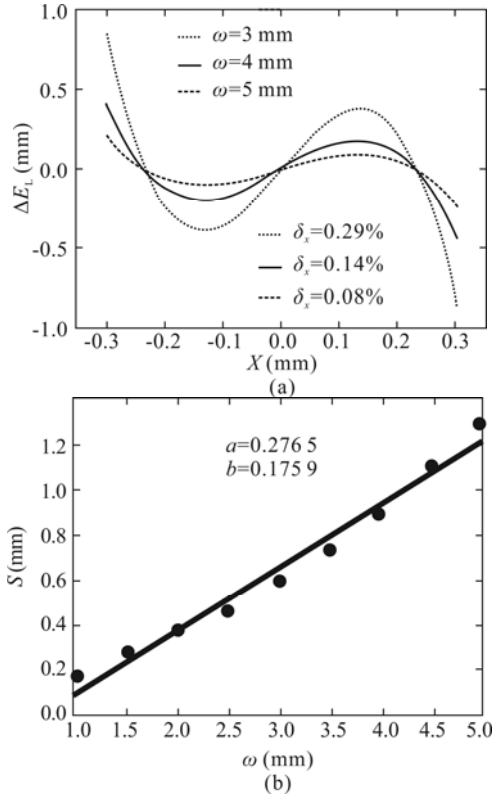

Fig.3 (a) Simulation results of the beam spot position measurement errors; (b) Relationship between measurement range of QD and the spot radius when the linearity is supposed to be 1%

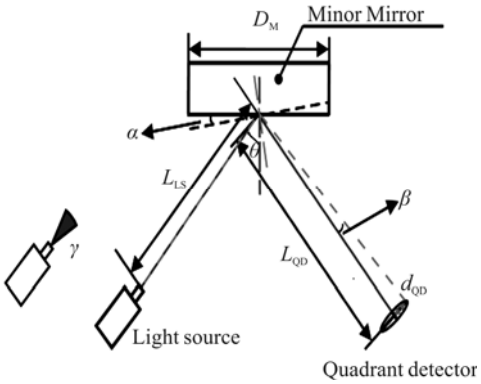

Fig.4 Working principle of the DADS

Tab.1 Parameters of the DADS

Symbol	Parameter
D_M	Diameter of the minor mirror
γ	Divergence angle of the LS
α	Absolute value of deflection angle of the minor mirror
θ	Angle between the beam emitted from the LS and normal of the minor mirror
β	Deflection angle of the beam reflected from minor mirror
L_{LS}	Distance between LS and minor mirror
L_{QD}	Distance between minor mirror and the QD
d_{QD}	Range of the spot center moving on the QD

For a certain size of QD, the relationship between linearity and corresponding measurement range has been analyzed. If the movement linearity of VCAs and the errors of fabrication are ignored, the linearity of FSM is regarded as that of the QD. Therefore, in order to achieve relatively high linearity of FSM system, the space of spot center moving on the QD should be no larger than the measurement range of QD, namely

$$d_{QD} \le S_W, \tag{5}$$

where S_W is the measurement range of the QD, and its approximate value can be obtained with a certain linearity by Eq.(3). Besides, the incident spot radius on minor mirror is $L_{LS}\times\tan\gamma$. To ensure the integrity of the spot illuminating on the minor mirror, the diameter of the minor mirror (D_M) should be bigger than that of the spot ($D_M \geqslant L_{LS}\times\tan\gamma$). And the spot radius on QD is given by

$$\omega_{QD} = \omega_0 + \left(L_{LS} + L_{QD}\right) * \tan\frac{\gamma}{2}. \tag{6}$$

Generally, in order to ensure the normal working of QD, the spot is not allowed to be beyond the edge of QD, otherwise, it introduces a relatively large position measurement error[11]. The spot radius arriving on QD should satisfy the inequality below

$$d_{QD} + \omega_{QD} \le R_{QD}, \tag{7}$$

where R_{QD} is the radius of QD. For the convenience of analysis for DADS, the L_{LS} and L_{QD} will be conformed to follow the approximate relationship of $L_{LS}=L_{QD}=L$. Then, substituting Eqs.(3)—(5) into Eq.(6) and Eq.(7) respectively, we can obtain

$$\begin{cases} \tan(2\alpha) \le \dfrac{R_{QD} - \omega_0 - 2L * \tan\dfrac{\gamma}{2}}{L}, \\ \tan(2\alpha) \le \dfrac{a\left(\omega_0 + 2L * \tan\dfrac{\gamma}{2}\right) - b}{L}, \end{cases} \tag{8}$$

where L is half of the total optical path length. And they are the mathematical models about the deflection angle and linearity (a, b) of FSM, divergence angle of LS, optical path length and the radius of QD. It is demonstrated that the deflection angle and linearity are constrained with each other.

Utilizing the mathematical model above, we will discuss the effects of the optical path length and divergence angle of LS on the deflection angle and linearity of FSM. A 7-mm-diameter QD is also used for the simulation and analysis below.

On one hand, if the linearity and optical path length are supposed to be 1%, 8 mm and 10 mm, respectively, the curves of deflection angle of FSM and divergence angle of LS are obtained in Fig.5(a). The solid lines are drawn according to the first inequality of Eq.(8), and the dotted line is drawn based on the second inequality of Eq.(8). The grey area is bounded by them, which stands for the

values of deflection angle and divergence angle which are able to satisfy the linearity above, and there is a largest deflection angle and the corresponding divergence angle in this area. It can be seen from Fig.5(a) that the relatively large deflection angle can be obtained by increasing the divergence angle and optical path.

On the other hand, if the deflection angle is kept as 2° and the values of linearity are 1%, 0.7% and 0.5%, respectively, the ranges of divergence angle and optical path length can be acquired according to Eq.(8), as shown in Fig.5(b). It can be easily seen that the first inequality is independent of the linearity, and the inequality is described as the dashed curve in Fig.5(b). However, the second inequality is related to the linearity, and other three solid curves can be achieved which correspond to the three values of linearity above. It is illustrated that the range area bounded by divergence angle and optical path length is S_1+S_2+S_3 when the linearity of QD is 0.5%, while its area is only S_1 when the linearity of QD is 1%. For each value of linearity, a maximum optical path length can be designed and an LS with minimum divergence angle can be chosen. Therefore, with the increase of linearity, the minimum divergence angle becomes smaller and the maximum optical path length becomes longer, simultaneously.

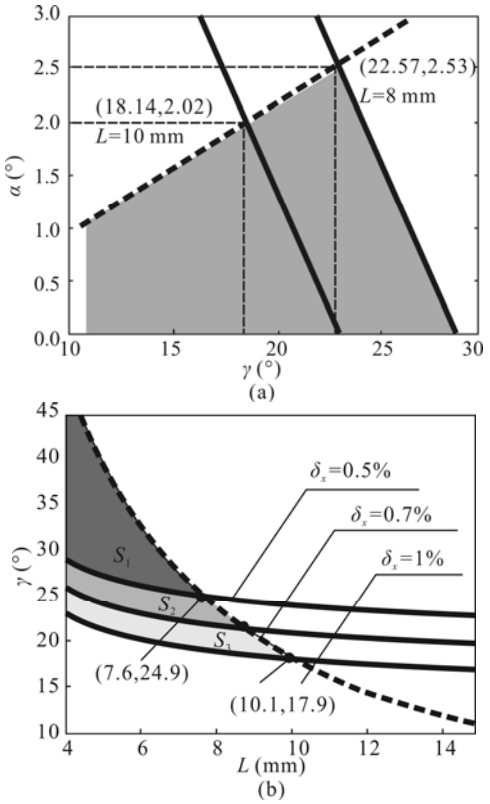

Fig.5 (a) The relationship between *α* and *γ* with 8 mm optical path length and 10 mm optical path length; (b) The relationship between *γ* and *L* when the linearity is different and deflection angle is kept constant

According to the analysis of two aspects above, the method of seeking optimal deflection angle and linearity of FSM has been demonstrated. By changing optical path length and divergence angle, the largest deflection angle can be obtained with a certain linearity, and a higher linearity can also be achieved with a certain deflection angle. Above all, the optimal deflection angle and linearity of FSM can be achieved.

In order to prove that this method is feasible in experiments, the following reasonable parameters are chosen: an available QD is employed (QP50-6 TO8S, 7.8 mm detector diameter and 0.042 mm gap), the optical path length is 5 mm to acquire the largest deflection angle, and the corresponding divergence angle of LS is about 35°. Then, we can design the FSM as shown in Fig.6(a) and set up the platform as shown in Fig.6(b).

The optical collimator is Leica-TPS600, of which the accuracy is 0.1″. The beam emitted by the optical collimator arrives at it again after being reflected by the mirror of the FSM. The mirror of the FSM is driven by the VCAs to deflect a corresponding mirror when a certain drive voltage is input. The spot moving on the surface of the optical collimator will not coincide with the initial spot. So, the deflection angle range of the FSM can be measured according to the spot displacement on the surface of the optical collimator. The deflection angle of our FSM is about ±2° along two axes by the optical collimator, as shown in Tab.2.

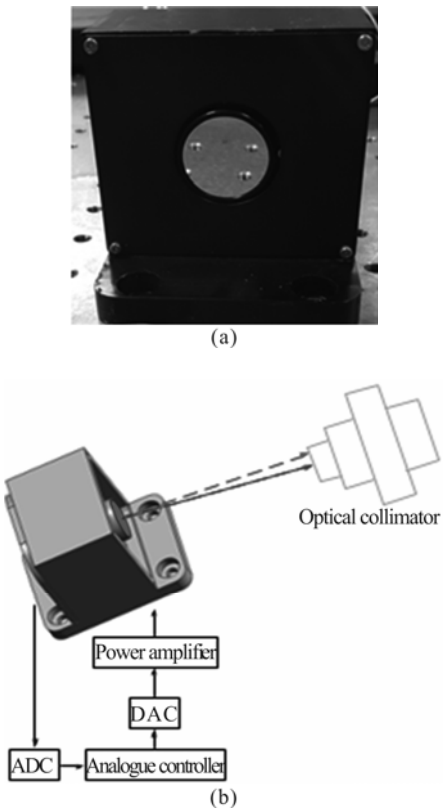

Fig.6 (a) The photograph of the QD-based FSM; (b) The diagram of the test platform for evaluating the deflection angle and linearity of the QD-based FSM

Tab.2 Comparison on parameters of several FSMs

FSMs	Deflection angle	Linearity
Ref.[3]	±1.125° (*x* axis) ±2.5° (*y* axis)	2.6% (two axes)
Ref.[12]	±1.5° (two axes)	1% (two axes)
Ref.[13]	±17.48′ (two axes)	4.89% (two axes)
This paper	±2.0° (two axes)	0.72% (*x* axis) 0.68% (*y* axis)

Driving the mirror of the FSM along the *x* and *y* axes in 0.02° step within the whole deflection angle, we can record the angle data in every position of the mirror by the optical collimator. And then the linearity can be calculated based on the obtained data, the deflection angle of FSM is about ±2° and the linearity are 0.72% (*x* axis) and 0.68% (*y* axis), as shown in Tab.2. Moreover, Tab.2 shows the parameters of several FSMs. It can be seen that the linearity of our QD-based FSM is better than that of others. Although the deflection angle of our QD-based FSM is slightly less than that of Ref.[3] along *y* axis, it is much larger than that of other FSMs. Above all, the FSM using the QD to detect angle can achieve good performance. Therefore, this method provides the theoretical guidance for design of large deflection angle and high linearity FSMs.

In conclusion, the DADS based on QD has been studied in detail. And the mathematical model describing the DADS has been established by analyzing the principle of position detecting and error characteristics of QD. On the basis of this model, we have simulated the relationships between deflection angle, linearity of FSM and parameters of the DADS. And the results show that the large deflection angle and high linearity can be achieved by decreasing the optical path length and increasing the divergence angle. Thus, the QD-based FSM can be optimized in this method. And it can be seen that our FSM achieves better performance than some other FSMs. In addition, this method can also be applied in other engineering practices.

References

[1] CHEN En-guo, HUANG Jia-min, GUO Tai-liang and WU Reng-mao, Optoelectron. Lett. **13**, 0253 (2017).
[2] M. R. Suite, H. R. Burris, C. I. Moore, M. J. Vilcheck, R. Mahon, C. Jackson, M. F. Stell, M. A. Davis, W. S. Rabinovich, W. J. Scharpf, A. E. Reed and G. C. Gilbreath, Proc. SPIE **5160**, 439 (2004).
[3] XUE Ting, ZHANG Shao-jie and WU Bin, Optoelectron. Lett. **13**, 0071 (2017).
[4] R. Gloess and B. Lula, Proc. SPIE **7739**, 77391U (2010).
[5] D. J. Kluk, M. T. Boulet and D. L. Trumper, Mechatronics **22**, 257 (2012).
[6] A. Berta, L. Hedding, C. Hoffman and M. Messaros, SPIE Design and Application **3787**, 181 (1999).
[7] J. M. Hilkert, G. Kanga and K. Kinnear, Proc. SPIE **9076**, 90760F (2012).
[8] A. J. Mäkynen, J. T. Kostamovaara and R. A. Myllylä, Proc. SPIE **1194**, 243 (1989).
[9] J. Zhang, M. A. Itzler, H. Zbinden and J.-W. Pan, Light: Sci. Appl. **4**, e286 (2015).
[10] S. Cui and Y. C. Soh, Appl. Phys. Lett. **96**, 081102 (2010).
[11] M. W. Chen, Y. P. Yang and X. T. Jia, Optik **124**, 6806 (2013).
[12] Optics In Motion (OIM), www.opticsinmotion.net.
[13] F. Chu, Ph.D. thesis, Changchun Institute of Optics, Fine Mechanics and Physics, Chinese Academy of Science, 115 (2017).